

# QCD measurements in the forward region at LHCb

Cédric Potterat, on behalf of the LHCb collaboration

*Departament de Estructura i Constituents de la Matèria, Universitat de Barcelona, Barcelona, Spain*

The LHCb experiment does have a unique pseudorapidity coverage in the forward region among the LHC detectors. Due to its unique angular range, it can provide QCD measurements complementary to the other LHC experiments. The measurement of the ratio of prompt  $\chi_c$  to  $J/\psi$  production, the measurement of  $\psi(2S)$  meson production, the observation of double charm production are presented. The charge track distribution at  $\sqrt{s} = 7$  TeV and the ratio of anti-proton to proton production at  $\sqrt{s} = 7$  TeV and 900 GeV are also reported.

## 1 Introduction

The LHCb experiment is dedicated to the  $b$ -hadron sector and aims to study CP-violation processes and rare decays involving  $b$  and  $c$  hadrons. The  $b\bar{b}$  pair production are strongly correlated at small angle with respect to the beam line, therefore the LHCb detector<sup>1</sup> has been designed as a single-arm forward spectrometer covering a pseudo-rapidity range  $2 < \eta < 5$ . The detector consists of a silicon vertex detector, a dipole magnet, a tracking system, two ring-imaging Cherenkov (RICH) detectors, a calorimeter system and a muon system.

## 2 Measurement of the ratio of prompt $\chi_c$ to $J/\psi$ production at $\sqrt{s} = 7$ TeV

The prompt production of charmonium  $\chi_c$  and  $J/\psi$  is studied<sup>2</sup> in  $pp$  collision at  $\sqrt{s} = 7$  TeV using an integrated luminosity of  $36 \text{ pb}^{-1}$  recorded by LHCb. The ratio of prompt  $\chi_c$  to  $J/\psi$ ,  $\sigma(\chi_c \rightarrow J/\psi\gamma)/\sigma(J/\psi)$ , is determined as a function of the  $p_T^{J/\psi}$  in the range  $2 < p_T^{J/\psi} < 15 \text{ GeV}/c$ . The  $\chi_c$  particles are reconstructed through the  $J/\psi\gamma$  channel. The  $J/\psi$ 's are selected using the dimuon channel and the photons are reconstructed in the calorimeter.

Since we measure the ratio of cross sections, many systematic uncertainties cancel. The gamma efficiency is the main difference entering the ratio calculation. It has been determined on Monte Carlo (MC) and validated on data using the ratio of two siblings channels:  $B^+ \rightarrow J/\psi K^+$  and  $B^+ \rightarrow \chi_c K^+$ , including charge conjugate. The candidates are selected keeping as many of the selection criteria in common as possible with the main analysis.

The ratio,  $\sigma(\chi_c \rightarrow J/\psi\gamma)/\sigma(J/\psi)$ , is in agreement with the NLO NRQCD<sup>4</sup> calculations over the full  $p_T^{J/\psi}$  range as shown in Fig. 1. This measurement is complementary from the cross-section ratio  $\sigma(\chi_{c2})/\sigma(\chi_{c1})$  for prompt production measured by LHCb<sup>5</sup> also shown in Fig. 1.

The polarization was not simulated in the  $\chi_c$  and  $J/\psi$  MC samples, thus a systematic uncertainty has been computed using all the possible configurations for both decays and is shown separately from other uncertainties in Fig. 1.

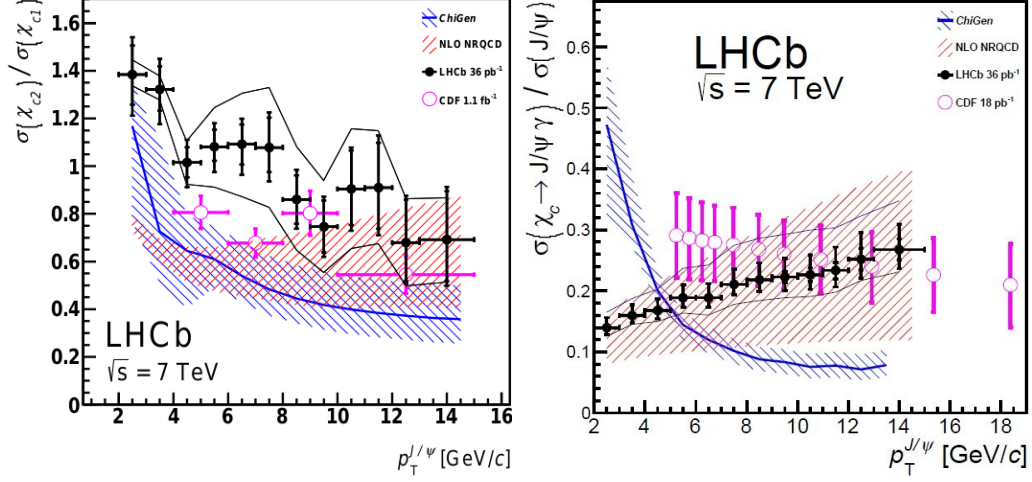


Figure 1: (Left) Ratio  $\sigma(\chi_{c2})/\sigma(\chi_{c1})$  and (Right) ratio  $\sigma(\chi_c \rightarrow J/\psi\gamma)/\sigma(J/\psi)$  in bins of  $p_T^{J/\psi}$  in the range  $2 < p_T^{J/\psi} < 15$  GeV/c. The LHCb results, in the rapidity range  $2.0 < y^{J/\psi} < 4.5$  and assuming the production of unpolarized  $J/\psi$  and  $\chi_c$  mesons, are shown with solid black circles and the error bars correspond to the statistical and systematic uncertainties (apart from the polarization). The lines surrounding the data points show the maximum effect of the unknown  $J/\psi$  and  $\chi_c$  polarizations on the result. The CDF data points, at  $\sqrt{s} = 1.96$  TeV in  $p\bar{p}$  collisions and in the  $\eta$  pseudo-rapidity range  $|\eta^{J/\psi}| < 1.0$ , are shown in with open pink circles. The two hatched bands correspond to the ChiGen Monte Carlo generator<sup>3</sup> and NLO NRQCD<sup>4</sup> predictions.

### 3 Measurement of $\psi(2S)$ meson production at $\sqrt{s} = 7$ TeV

The differential cross-section for the inclusive production of  $\psi(2S)$  mesons in  $pp$  collisions at  $\sqrt{s} = 7$  TeV has been measured<sup>6</sup> using an integrated luminosity of  $36 \text{ pb}^{-1}$ . The decay channels  $\psi(2S) \rightarrow \mu^+\mu^-$  and  $\psi(2S) \rightarrow (J/\psi \rightarrow \mu^+\mu^-)\pi^+\pi^-$  are reconstructed using prompt  $\psi(2S)$  and  $\psi(2S)$  decaying from a  $b$ -hadron (delayed). The separation between the two samples is done using a pseudo-decay-time distribution defined as  $t = d_z(M/p_z)$ , where  $d_z$  is the separation along the beam axis between the  $\psi(2S)$  decay vertex and the primary vertex,  $M$  is the nominal  $\psi(2S)$  mass and  $p_z$  is the component of its momentum along the beam axis. The polarization of promptly reconstructed  $\psi(2S)$ 's is not measured here, therefore a systematic uncertainty is computed separately for the unknown state of the polarization. This does not effect the delayed  $\psi(2S)$ .

The differential cross-sections for prompt  $\psi(2S)$  and delayed  $\psi(2S)$  mesons are measured in the kinematic range  $p_T(\psi(2S)) \leq 16$  GeV/c and  $2 < y(\psi(2S)) \leq 4.5$ :

$$\sigma_{\text{prompt}}(\psi(2S)) = 1.44 \pm 0.01(\text{stat}) \pm 0.12(\text{sys})_{-0.40}^{+0.20}(\text{pol}) \mu\text{b}$$

$$\sigma_b(\psi(2S)) = 0.25 \pm 0.01(\text{stat}) \pm 0.02(\text{sys}) \mu\text{b}$$

Recent QCD calculation on the differential cross-sections are found to be in a good agreement with these results as shown in Fig. 2. Combining this result with the LHCb  $J/\psi$  measurement, the inclusive branching ratio has been determined to be:

$$\mathcal{B}(b \rightarrow \psi(2S)X) = (2.73 \pm 0.06(\text{stat}) \pm 0.16(\text{syst}) \pm 0.24(\text{BR})) \times 10^{-3}$$

where the last uncertainty is due to the  $\mathcal{B}(b \rightarrow J/\psi X)$ ,  $\mathcal{B}(J/\psi \rightarrow \mu^+\mu^-)$  and  $\mathcal{B}(\psi(2S) \rightarrow e^+e^-)$  branching fraction uncertainties. The later branching fraction is used and justified by the leptons universalities.

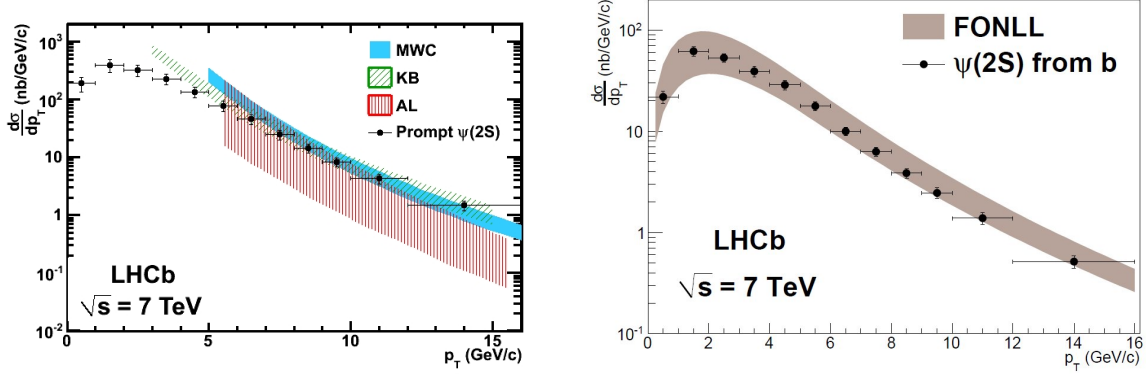


Figure 2: (Left) Differential production cross-section vs.  $p_T$  for prompt  $\psi(2S)$ . The predictions of three non-relativistic QCD models are also shown for comparison. MWC<sup>7</sup> and KB<sup>8</sup> are NLO calculations including colour-singlet and colour-octet contributions. AL<sup>9</sup> is a colour-singlet model including the dominant NNLO terms. (Right) Differential production cross-section vs.  $p_T$  for delayed  $\psi(2S)$ . The shaded band is the prediction of a FONLL calculation<sup>10</sup>.

#### 4 Observation of double charm production involving open charm

The production of a  $J/\psi$  accompanied by open charm and pairs of open charm (C) hadrons are observed<sup>11</sup> in  $pp$  collisions at  $\sqrt{s} = 7$  TeV using an integrated luminosity of  $355 \text{ pb}^{-1}$ . Leading order calculation in perturbative QCD and Double Parton Scattering (DPS) predictions<sup>12,13</sup> give significantly different prediction,  $\sigma(J/\psi C + J/\psi \bar{C}) \sim 18 \text{ nb}$  and  $\sim 280 \text{ nb}$  respectively. The DPS predictions can also be tested through the ratios of cross sections of the charm hadrons involved: in a DPS scenario  $\sigma(C_1) \times \sigma(C_2) / \sigma(C_1 C_2)$  should be equal (twice bigger if  $C_1 \neq C_2$ ) to the effective DPS cross-section measured at the Tevatron<sup>14</sup>.

The open charm hadrons considered here are:  $D^0$ ,  $D^+$ ,  $D_s^+$  and  $\Lambda_c^+$ , while the  $C\bar{C}$  are used as control channels. Selected charged tracks are combined to form  $J/\psi \rightarrow \mu^+ \mu^-$ ,  $D^0 \rightarrow K^- \pi^+$ ,  $D^+ \rightarrow K^- \pi^+ \pi^+$ ,  $D_s^+ \rightarrow K^- K^+ \pi^+$  and  $\Lambda_c^+ \rightarrow p K^+ \pi^+$ . Subsequently these candidates are combined into  $J/\psi C$ ,  $CC$  and  $C\bar{C}$ . The combinations are requested to come from the same primary vertex and in the rapidity range  $2 < y^{J/\psi, C} < 4$  while the  $p_t^{J/\psi} < 12 \text{ GeV}/c$  and  $3 < p_t^C < 12 \text{ GeV}/c$ . In addition a flight distance  $c\tau > 100 \mu\text{m}$  is required for the C.

Signals with a statistical significance over five standard deviations have been observed for the four  $J/\psi C$ , for six  $CC$  modes:  $D^0 D^0$ ,  $D^0 D^+$ ,  $D^0 D_s^+$ ,  $D^0 \Lambda_c^+$ ,  $D^+ D^+$  and  $D^+ D_s^+$ , and for seven  $C\bar{C}$  channels:  $D^0 \bar{D}^0$ ,  $D^0 D^-$ ,  $D^0 D_s^-$ ,  $D^0 \bar{\Lambda}_c^-$ ,  $D^+ D^-$ ,  $D^+ D_s^-$  and  $D^+ \bar{\Lambda}_c^-$ .

In Fig. 3 the cross-sections are shown on the left and the DPS fraction on the right. Results favour the DPS model using the effective cross-section measured at Tevatron, which is also favoured with the absence of azimuthal and rapidity correlations.

The transverse momentum of these events has also been studied. In the  $J/\psi C$  case we can see an harder  $p_T^{J/\psi}$  spectra compared to the prompt  $J/\psi$  production.

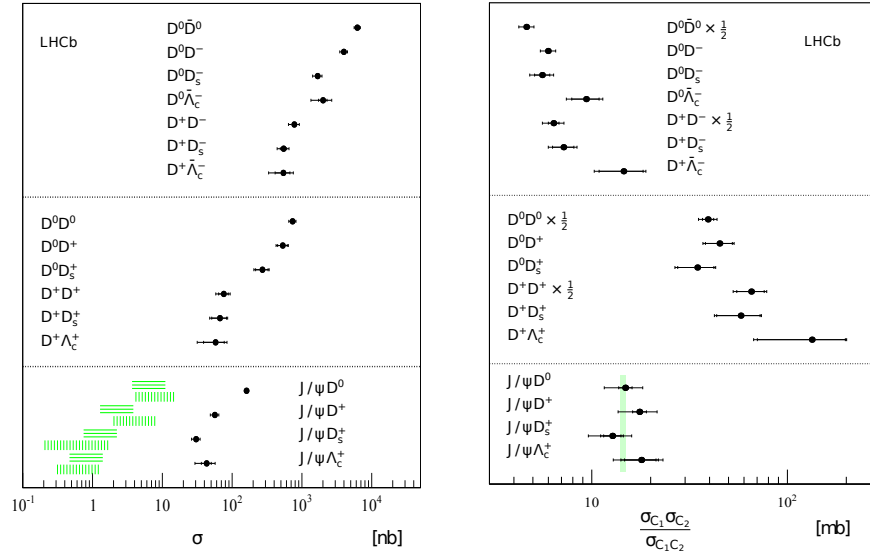


Figure 3: (Left) Measured cross-sections  $\sigma_{J/\psi C}$ ,  $\sigma_{CC}$  and  $\sigma_{C\bar{C}}$  (points with error bars) compared, in  $J/\psi C$  channels, to the calculations in Refs. <sup>15</sup> (vertical hatched areas) and Ref. <sup>16</sup> (horizontal hatched areas). The inner error bars indicate the statistical uncertainty whilst the outer error bars indicate the sum of the statistical and systematic uncertainties in quadrature. (Right) Measured ratios  $\sigma_{C_1 \sigma_{C_2}} / \sigma_{C_1 C_2}$  (points with error bars) in comparison with the expectations from DPS using the cross-section measured at Tevatron for multi-jet events (light green shaded area). For the  $D^0 D^0$ ,  $D^0 \bar{D}^0$ ,  $D^+ D^+$  and  $D^+ D^-$  cases the ratios are rescaled with the symmetry factor of one half. The inner error bars indicate the statistical uncertainty whilst the outer error bars indicate the sum of the statistical and systematic uncertainties in quadrature. For the  $J/\psi C$  case the outermost error bars correspond to the total uncertainties including the uncertainties due to the unknown polarization of the prompt  $J/\psi$  mesons.

## References

1. LHCb collaboration, JINST **3**, S08005 (2008)
2. LHCb Collaboration, arXiv:1204.1462
3. L. A. Harland-Lang and W. J. Stirling, <http://projects.hepforge.org/superchic/chigen.html>
4. Y.-Q. Ma, K. Wang, and K.-T. Chao, Phys. Rev. D **83**, 111503 (2011)
5. LHCb Collaboration, arXiv:1202.1080
6. LHCb Collaboration, arXiv:1204.1258, submitted to EPJ
7. Y.-Q. Ma, K. Wang and K.-T. Chao, arXiv:hep-ph/1012.1030
8. B. Kniehl and M. Butenschön, Phys. Rev. Lett **106**, 022003 (2011)
9. Phys. Rev. Lett **101**, 152001 (2008) and Eur. Phys J. C **61**, 693 (2009)
10. JHEP **9805**, 007 (1998) and JHEP **0407**, 033 (2004)
11. LHCb Collaboration, arXiv:1205.0975, submitted to JHEP
12. Phys. Rev. D **57**, 4385 (1998) and Phys. Rev. D **73**, 074021 (2006)
13. Phys. Rev. Lett. **107**, 082002 (2011), Phys. Rev. B **705**, 116 (2011), arXiv:1106.2184 and arXiv:1111.3255
14. CDF collaboration Phys. Rev. D **56**, 3811 (1997)
15. Phys. Rev. D **57**, 4385 (1998) and Phys. Rev. D **73**, 074021 (2006)
16. J.-P. Lansberg, Eur. Phys. Rev. J. C **61**, 693 (2009)